

Study of The Microstructure of Aisi Steel 304l in wz, Haz And Bm After Welding in the Gmaw Process

*Queiroz, A, V.¹Fernandes, M, T. ²Silva, L,M. ³Demarque, R. ⁴Oliveira,E.M. ⁵Ellem, P.S. ⁶Lima, I,R. ⁷Barbosa, G, C. ⁸Teixeira, P, S. ⁹Castro, J.A. ¹⁰

Corresponding Author: Queiroz, A, V.1Fernandes

Abstract: In this work, it was qualitatively measured the microstructure of the HAZ (Heat Affected Zone) and WZ (Weld Zone) of AISI 304L Stainless Steel by the GMAW (Gas Metal Arc Welding) process pulsed, using the single bead-on-plate procedure. For this purpose, was used GMAW process (Gas Metal Arc Welding) was in single pass deposition on plate of this steel 304L. After the welding process it was observed that the transfer occurred (metal transfer) exercised important effect on some on some properties of the weld joint, such as directing of the grains, inter dendritic spacing and microhardness Vickers during the welding. In the Centre of the weld bead, heat flow and dendritic structures and the microstructure is predominantly ferrite δ and with austenitic lines because the steel is predominantly austenitic. Growth in weld joints is, being an epitaxial phenomenon, where the grains of the WZ increase with the same crystalline orientation of the grains of the HAZ, as if the grains were planted in BM.

Keywords: Weld, process GMAW, dendrites, heat flow.

Date of Submission: 12-01-2018

Date of acceptance: 27-01-2018

I. INTRODUCTION

Stainless steels are part of an important class of materials having a large field of application, which is conferred on them due to combinations of characteristics that austenitic steels exhibit such as: corrosion resistance, ductility, toughness, weldability and mechanical strength at temperatures high. However, its properties when it is subjected to a rigorous thermal cycle, as in the case of a welding process, undergo significant qualitative and quantitative changes. These must be carefully checked so as not to compromise the application of the welded material. In order to perform this control it is necessary to know well the dynamics of the transformations that occur in the material when welded, due to temperature gradients, phase transformations, refining and grain growth. In recent years, has been developed many studies on welding of Steel AISI 304L, for example, [1],[2] studied the ZF microstructure in FZ after welding process, It was observed that the dimensions of the BM, HAZ and WZ have been proportionate to the increased heat input, studied thermal effects by numerical modeling via finite volumes [3,4]. This model featured large efficient by studying the thermal cycle. In this work the aim was to analyze the metallographic structure, dendritic structure in WZ and Vickers microhardness on a contribution fixed thermal areas in different regions BM, WZ and HAZ. However, the results presented concerning the study of the influence of the thermal contribution on weld joint properties of these materials when welded by the GMAW process with pulsed metal transfer modes are very limited. This is the main technological objective of this study, to contribute significantly and reliably with the changes in the properties and characteristics of the welded material against the material as received.

II. MATERIALS AND METHODS

The material used in the experimental welding process were in plates for each austenitic stainless steel AISI 304L and arame de adición ER316L. Tables 1 and 2 respectively show the chemical analysis and dimensions of the plates analyzed.

Table 1 - Chemical Composition (% By Weight) Of Stainless Steel AISI 304L and Chemical Composition Of The Addition Wire ER316L According ESAB (2005) (% By Weight).

Element	% Weigh
C	0,017
Mn	1,170
Si	0,486
P	0,043

S	0,003
Cr	18,420
Ni	8,080
Mo	0,003
Cu	0,031
N	0,062

Table 2 - Dimensions of sheets of austenitic stainless steel AISI 304L.

AISI	Length[mm]	Width [mm]	Thickness [mm]
304L	175	50	9

In this work, was used the GMAW welding process (Gas Metal Arc Welding) with metal transfer by pulsed spray equipment using the synergic model MIG PULSE 4001 DP - Castolin Eutectic in the welding lab EEIMVR UFF. To control with greater rigidity the welding speed during the process, the welding torch is coupled to a mobile arc that has its speed controlled by a frequency inverter [4]. It was used for welding austenitic stainless steel AISI 304L and consisting of 98% argon shielding gas and 3% oxygen and adding ER316L wire with a diameter of 1.2mm. The welding plates was all in a single pass and deposition of additional material, forming a strand with an average length of 160 mm AISI 304L along the length of the plates. The thermal input of tracks are shown in Table 3. For this work use only heat supply in order to observe the formation of epitaxial grain, columnar inter dendritic pattern and microhardness Vickers in BM, HAZ and WB.

Table 3 - heat input range

Material [AISI]	Heat Input range HI* [kJ/mm]
STEEL 304L	1,3 – 1,7

In addition to the initial parameters related to the machine, cited above, there are other parameters initially set: The Table 4 shows the other welding parameters used in the welds of the AISI 304L steel.

Table 4 - Welding Parameters

Plate	504
Metal transfer mode	Spray Pulsed
Current [A]	239
Voltage [V]	26,6
Speed [mm/s]	6,72
Heat Input HI* [kJ/mm]	1,5

By capturing the current and voltage data during the welding heat input were calculated in Eq. 1.

$$HI = \frac{I \times V \times \eta}{v} \text{ (J/mm)} \quad (1)$$

After all the welding process, a sample was taken from each plate to perform the microstructural and macrostructural characterization, sizing FZ and HAZ, stretching grain and dendritic package. Posteriorly, polishing and attack Behara of the steel samples, the microstructural characterization was performed by Lentz optical microscope. The capture of micrographs was performed by a camera attached to the microscope that sends messages to the computer using the software Image Pro Plus 4.0. For the said steel solidification process after the welding process, the desired level of overheating was observed, i.e. 10% above the liquidus temperature which usually represents the degree of superheat adopted in the foundry industry. The Vickers average microhardness of the steel AISI 304L after the welding process of HAZ, FZ and BM were evaluated and displays a graph with the Microhardness Vickers values expressed in lines for the cross section of the plate.

1

III. RESULTS AND DISCUSSION

The Fig. 1 shows a cross-sectional view of different areas. As it can be seen WZ is mainly composed of columnar dendrites as shown in Fig. 1 (a) and (b), the rapid solidification is derived from the super-cooling which occurs at the solid / liquid interface in MIG / MAG that grows in the direction perpendicular to the edge of fusion line (FL).

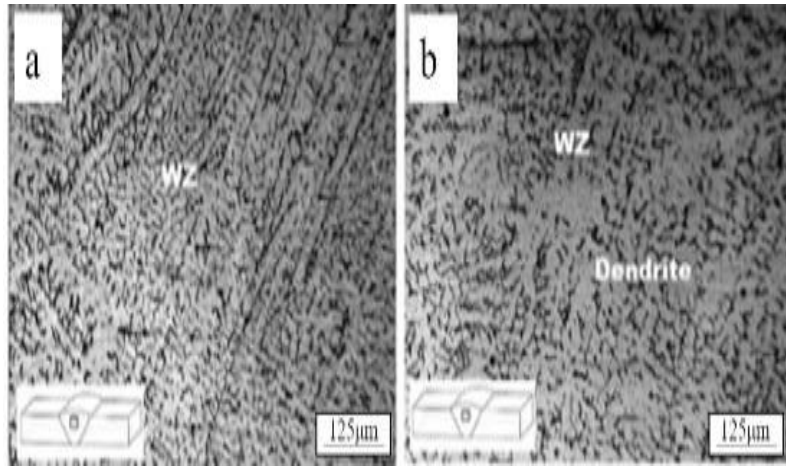


Figure 1. Microstructure of weld zone.

Figures 2 and 3 show the results experienced by two primary dendrite spaces as a solidification evolved. As such, they correspond to the equations tested and represent, respectively, the results of the spatial analysis as well as the temperature and rate of displacement of the liquidus isotherm. Foi used or expoente -0.43 e -0.44 for as leis de crescimento two referred españamentos. On ΔT , é or solidification interval for equilateral conditions, or spacing and given the primary dendritic crescimento emergência da coli de resfriamento is described in equation (2).

$$\lambda_1 = C * T_R^{-n} \quad (2)$$

Figure 3 shows the experimental results of the primary dendritic spacings as a function of the cooling rate. Said spacings also decrease to higher values of T_R . It also shows that the exponent -2.96, obtained for the case investigated, characterizes the growth law of the primary dendritic spacings with T_R . This behavior shows a very good agreement with the results obtained by [5] as well as [6] for alloys of several binary systems solidified in vertical upstream molds under transient heat extraction conditions. Analogously with cell growth, one can expect that the primary spacing dependent cooling rate

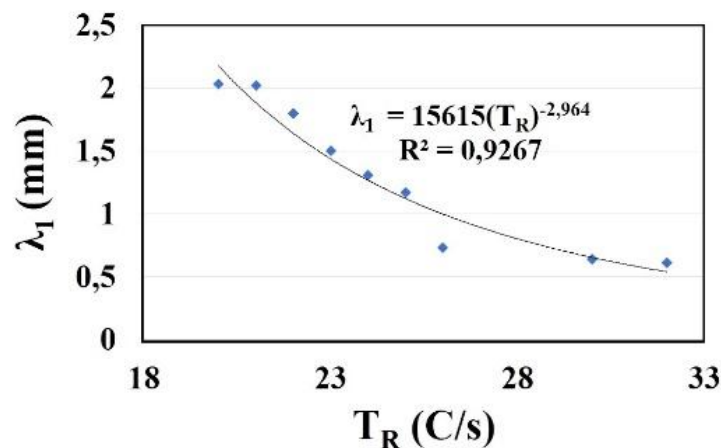


Figure 2 - Primary dendritic spacing as a function of position for the material studied.
(a) position ranging from 10 mm and (b) cooling rate.

The Figure 3 shows the experimental values of the primary dendritic spacings of the alloy investigated as a function of the velocity of displacement of the liquidus isotherm. It can be seen that the spacing in question decreases as V_L increases. In this case, the -0.66 exponent was determined for the analyzed material thus characterizing an experimental law for the primary dendritic spacings with V_L of the form $\lambda_1 = \text{constant} (V_L)^{-0.66}$. Whatever the conditions that allow the ends (tips) of the dendrites to be accelerated or increase their velocity relative to the roots, a coarser dendritic structure formed at high temperature should be favored.

The law of primary dendritic growth as a function of the velocity of displacement isotherm liquidus is described in Equation (3).

$$\lambda_1 = C * V_L^{-n} \quad (3)$$

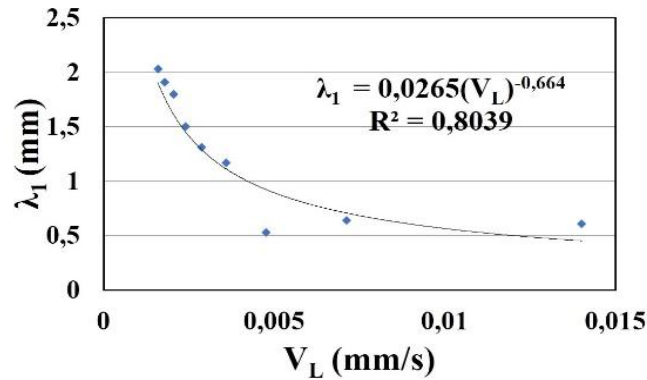


Figure 3 - Primary dendritic spacings as a function of the displacement velocity of the liquidus isotherm.

The Vickers micro-hardness on the surface WZ, HAZ and BM were measured and plotted in Fig. 5. Taking the base metal as its initial state, austenitic grain is obtained at the beginning. Due to the temperature gradient provided by the welding process the HAZ shows a steep slope in the hardness profile, due to the thermal cycle that caused a dissolution in the delta ferrite sites, thus initiating a reduction in the hardness profile against the base metal. The hardness profile in the melt zone can be divided into two parts, the first is the HAZ / WZ interface and the second the center of the weld bead. The first part presents a hardness similar to that presented in the HAZ, which can be explained by the fact that although this region was melted, it was more distant from the heat source so its cooling was smoother when compared to the second part, allowed as soon as the dendritic structure formed in the first part of the molten region grew to become coarser. The second part presents a significantly lower hardness than the base metal and the ZTA, a fact that can be justified by the location of this region being exactly where the heat source passed, that is, it suffered the highest temperature as soon as its cooling was more abrupt, giving time for dendritic structure to grow, remaining refined and thus reducing its hardness against the peripheral region of the WZ and BM. The microhardness Vickers on surface WZ, HAZ and BM was measured and plotted in Fig. 4. Furthermore although instabilities of the displayed values, is clear and continuous increase of the microhardness in the WZ in [7] fusion line, can also see that in HAZ is no variation in the microhardness, expected increase in microhardness Vickers due to the cooling of the material the hardness is highest close to BM and lower near WZ. Thus, this result can be explained as a result of the measurements made in the austenitic matrix, where the thickness of the ferrite dendrites δ is very thin, making it difficult to measure the Vickers microhardness. This result was similar to [8],[9].

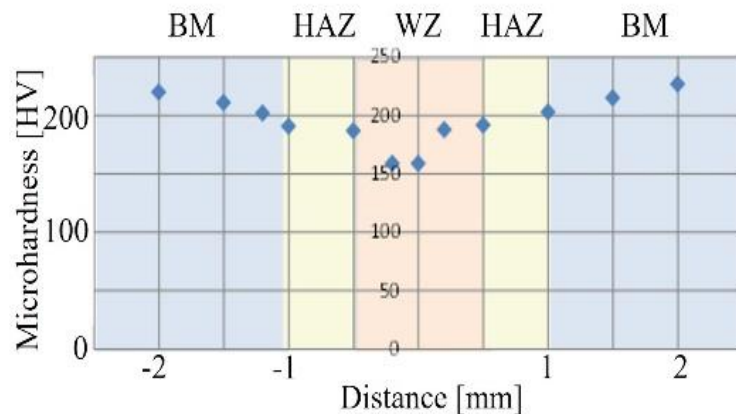


Figura4. Microhardness profile of the weldment.

The Fig. 5 show differences in grain formation, in the melt puddle due to the cooling time. The various cooling time is responsible for the refinement of the gross fusion structure, bringing benefits such as mechanical properties such as tensile strength, fracture and stress. The variation in time is in function of the cooling speed, causing changes in the microstructure. The grain structure is anisotropic, as it columnar form toward the heat flux approximately normal to the direction of welding, as [10].

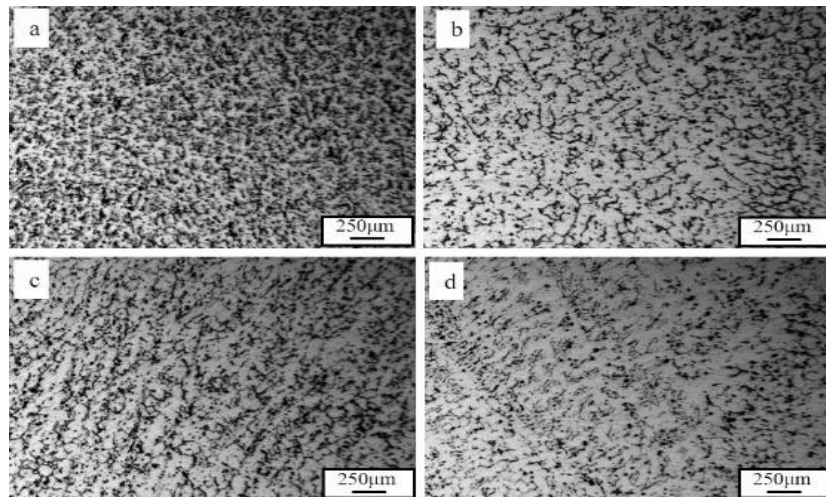


Figure 5 - Weld joint of Microstructure, (a) source, (b) center of FZ, (c) Around the weld bead, (d) Crest of the weld bead

The results discussed in this section are for the characteristics are mainly related to the reason $[Cr / Ni]_{eq}$ and the cooling rate. So, how to calculate $[Cr/Ni]$ (AISI 304 L) is 2.05, noted in the pseudobinary diagram of [2]. The calculated by chemical composition of the material. The reason ensures that the material has volume fraction of ferrite δ in austenitic matrix, an important factor is the cooling rate that will influence the amount of volume fraction ferrite δ , among other words if there is less heat will impose higher cooling rate, lower volume fraction δ ferrite and lower dendrite spacing. This approach is the same AISI steel 304L for the solidification of this material occurs according to the reaction $Liq \rightarrow L + \delta \rightarrow \delta + \gamma$, in Fig. 7, also observed in pseudobinary diagram of [2]. Whereas this steel remains for some time in the single-phase field ferrite δ , the lower the cooling rate, the material will stay in the field longer and the greater the fraction of ferrite δ in austenitic matrix. It can be seen that for increasing values of heat input has the growth of austenitic grains [2] and higher intakes imply lower cooling rates. In Fig. 6 was observed the maximum temperature 1600°C, liquid region, $L + \delta$ show formation of ferrite δ , phase δ responsible for solidification on the influence of the Cr e Ni (fracion $[Cr/Ni]_{eq}$) present in stainless steel and posteriorly there is phase $\delta + \gamma$. The formation of ferrite δ , phase ductil, it's not harmful to steel, because minimizes the effect of Cr and prevents corrosion.

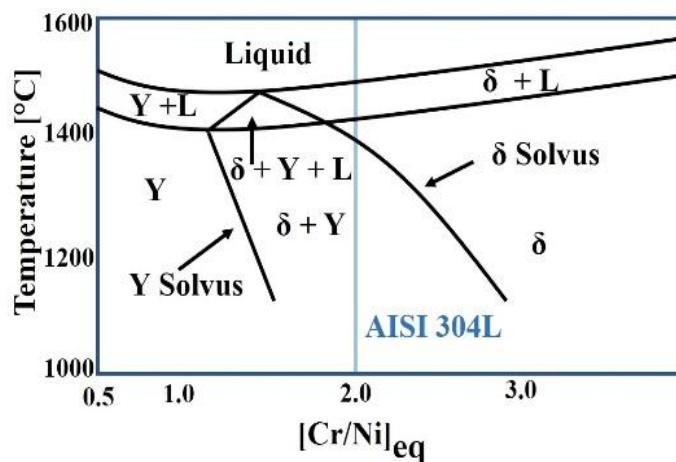


Figure 6 - Pseudo-binary diagram of the Fe $[Cr-Ni]_{eq}$ system in the blue line referring to the $[Cr / Ni]_{eq}$ ratio for the AISI 304L [2].

IV. CONCLUSIONS

With the object of studying the dendritic structure and with the purpose of analyzing the effect of transformations during the welding, in different conditions under the following conditions: The dendritic structure and / or the heat flow in the ZF is perpendicularly formed at the root of the weld and solder ridge and the center of the weld bead has a slight curvature along their sides; growth in solder joints is epitaxial, is a phenomenon where the grains of WZ grow with the same crystal orientation of the grains of the HAZ. Thus, each new grains solidifies in the same crystallographic direction of the grains of HAZ.

REFERENCES

- [1]. Demarque, R., Castro, J.A., Xavier, C.R., Almeida, D.S.S., Marcelo, C.J., Queiroz, A.V., Numerical and Experimental Study of the Properties of Welded Joints of Rebar by MIG, XLI CONSOLDA – Congresso Nacional de Soldagem, ABS, Salvador-BA, Brasil, 2015.
- [2]. Ronqueti, L.A., Effect of the metal transfer mode on the thermal and metallurgical changes behavior in GMAW welding of AISI 304 and 316 austenitic steels used in nuclear facilities, master's thesis, Indústrial Metallurgical Engineering School of Volta Redonda, PPGEM, UFF, p 1-163, 2014.
- [3]. Almeida, S.S., Experimental and numerical evaluation of weldability of 2205 duplex stainless steels and superduplex 2507, master's thesis, Indústrial Metallurgical Engineering School of Volta Redonda, PPGEM, UFF, p 1-147, 2014.
- [4]. Chandra, B.R., Arul, S., Sellamuthu, R., Effect the electrode diameter and input current on gas tungsten arc welding heat distribution parameters, Procedia Materials Science 5, p 2369-2375, 2014.
- [5]. Nogueira, M.R., Carvalho, D.B., Moreira, A.L., Dias Filho, J.M., Rocha, O.L., Espaçamentos dendríticos primários da liga Sn-5%Pb solidificada direcionalmente em um sistema horizontal, Revista matéria, V17, N.2, ISSN 1517-7076 artigo 11472, pp.1009-1023, 2012.
- [6]. ROCHA, O.L., SIQUEIRA, C.A., GARCIA, A., "Cellular/dendritic transition during unsteady-state unidirectional solidification of Sn-Pb alloys", *Materials Science and Engineering A*, v. 347, pp. 59-69, 2003.
- [7]. Razavi, R.J., Laser beam welding of Waspaloy: Characterization and corrosion behavior evaluation, Optics & Laser Technology B2 p 113-120, 2016.
- [8]. Santos, E.P., Demarque, R., Castro, J.A., Queiroz, A.V., Silva, L.M., Silva, R.S., Xavier, C.R., Comparative study of the microstructural and thermomechanical transformations of welded joints of AISI 316 and AISI 316L Steel by the TIG Autogenous process, XLIII CONSOLDA – Congresso Nacional de Soldagem, Joinville, Brasil, 2017.
- [9]. Demarque, R., Santos, E.P., Castro, J.A., Queiroz, A.V., Silva, L.M., Silva, R.S., Xavier, C.R., Comparative evaluation of microstructural and metallurgical transformations of welded joints of AISI 316L Steel by the GMAW process and autogenous GTAW, XLIII CONSOLDA – Congresso Nacional de Soldagem, Joinville, Brasil, 2017.
- [10]. Lima, I.L., Silva, G.M., Chilque, A.R.A., Schwartzman, M.M., Bracarense, A.Q., Quinan, M.A.D., Microstructural characterization of dissimilar welds steel ASTM A-508 and AISI 316 l welding Insp. São Paulo, Vol. 15, N. 2. P 112-120, 2010.
- [11]. Lippold, J.C., Varol, I., Baeslack, W. A. Microstructural evolution in duplex stainless steel weldments. Proceedings. In: Conference Duplex Stainless Steels'91, Les Éditions de Physique: v. 1, p. 383-391, 1991.

Queiroz, A, V. I. Fernandes. "Study of The Microstructure of Aisi Steel 304l In Wz, Haz And Bm After Welding in The Gmaw Process." IOSR Journal of Engineering (IOSRJEN), vol. 8, no. 1, 2018, pp. 14-19.